Journal of Engineering and Sustainable Development
http://jeasd.uomustansiriyah.edu.iq/index.php
https://doi.org/10.31272/jeasd.26.1.10

Vol. 26, No. 01, January 2022
ISSN 2520-0917

PERFORMANCE OF DIFFERENT PHOTOVOLTAIC TECHNOLOGIES FOR AMORPHOUS SILICON (A-SI) AND COPPER INDIUM GALLIUM DI-SELENIDE (CIGS) PHOTOVOLTAIC MODULES

Noor Jamel Kadia[1] **Emad T. Hashim[1]** ***Oday I. Abdullah[1,2]**

1) Department of Energy Engineering, College of Engineering, University of Baghdad, Iraq
2) Hamburg University of Technology, Hamburg, Germany

Received 27/7/2021 ***Accepted in revised form 10/9/2021*** ***Published 1/1/2022***

Abstract: In this work, the analysis of performance of two types of photovoltaic (PV) (Amorphous Silicon (a-Si) Copper Indium Gallium Diselenide (CIGS) technologies were achieved out under under Iraqi (Baghdad)climate conditions. The elevation of the selected site is 9 m above ground level. The experimental work covered the eight commercially available PV technologies. The two technologies that employed in this work are, Amorphous Silicon (a-Si) and Copper Indium Gallium Diselenide (CIGS). The total period of the experimental work was 7 months, and the data were analyzed simultaneously. Special attention is given to the influence of temperature and solar radiation the performance of the PV modules. Where, it was proposed a simple I-V curve test for PV modules. The results showed that the proposed system successfully experimentally extracted I-V curves of the selected two PV modules (amorphous and CIGS solar modules). The maximum values of power (Pmax) at solar radiation intensity 750 W/m² are 2.742 W, and 2.831 W for amorphous silicon and copper indium gallium di-selenide respectively. This is occurred because the lowest solar module operating temperature (19 oC and 17 oC for solar radiation 750 and 1000 W/m2 respectively) and ambient temperature (7 oC) and for Jan., 2021 than other months. Consequently, the same behavior for the two modules at solar irradiance 1000 W/m2 with the highest power value; 2.680 W, and 3.198 W of amorphous silicon and copper indium gallium di-selenide respectively. Furthermore, the minimum values of power (Pmax) at solarradiation intensity 750 W/m² are 2.530, and 2.831 for amorphous silicon and copper indium gallium di-selenide respectively because we have the highest solar module operating temperature (57 oC, and 55 oC respectively) and ambient temperature (45 oC) for April, 2021 than other months. Consequently, the same behavior for the two modules at solar irradiance 1000 W/m2 with the highest power value; 2.680 W, and 3.198 W of amorphous silicon and copper indium gallium di-selenide respectively. The highest efficiency can be notes for CIGS solar module with a value 7.3%, while the lowest one is 5.5% for amorphous solar module.

Keywords: *performance*, *photovoltaic technology*, *I-V characteristic*, *P-V characteristic.*

1. Introduction

The process of converting the light falling on the earth from the sun and converting it into another form of energy (electrical energy) is called the photoelectric effect. Electron holes (a pair) are generated when photon energy is absorbed by the semiconductor material. When the energy of a photon is large enough, the charge carriers will move to a higher energy state. p-n junction is represented the Semiconducting materials, where it will collect these energetic charge carriers and lead to reduce the difficulties of their movement as electrical current. Generally, this is the typical

**Corresponding Author*: isam.abdullah@su.edu.krd

operation process of the photovoltaic solar cells. Where, the high efficiency of this process a significant impact in the market of global energy. Where for the Cu (InGa) Se2 or CIGS thin-film solar cell, the photovoltaic efficiency of conversion reached around 22.[1]

The commercial technologies that used in different applications to generate power are available are predominantly silicon-based. It can be classified as either crystalline silicon or thin film. Where, each type has specific characteristics and cost that is different from the other type.[2]

At present, the photovoltaic (PV) modules market consists of 90% conventional, diffused junction monocrystalline and polycrystalline silicon modules [3-5]. Also, there are other, more advanced types of PV modules in the market, but in a limited form. Where, it is expected that will spread more widely in the coming period such as the silicon heterojunction module that produced mainly by Panasonic.[6]

At the present time, there are many kinds of conversion technologies for solar energy that available. Where, it was used Solar-concentrators for thermal generation for long time, but last years it was used less and less. The reason behind this, is using the new kinds that has low risk and utility-scale photovoltaics. The technology of photovoltaics (Silicon wafer) was dominated on the market of solar panel for long time.

It can be considered the thin-film solar cells (TFSC) are the alternative one, where it was made with small thick (few microns). That is lead to enhance the collection of electron and small amount of material. It was designed TFSC's to be optimal absorbers with direct band-gaps that optimized for the solar spectrum. Where it works properly with the variation of temperature and it can be deposited on different types of surfaces. This is will lead to use it in a several applications. The new technology of deposition will reduce the cost and time of manufacturing. The current available thin-film technologies are CdTe, amorphous silicon (a-Si), and CIGS [7]. CIGS solar-cells have long produced the highest efficiency TFSCs. Katee et al. [8] investigated with detail work on extracting solar module I-V and P-V characteristic performance curves.

Tossa et al. [9] investigated the behavior of three different PV technologies under the environmental conditions of city (Burkina Faso). The the experimental results proved that the micromorph module has the optimal behavior with an average performance ratio of 92%. Where, it was done evaluation for the performance of six different PV technologies that installed in different regions in Brazil (with environmental conditions). It was found high degradation in areas with high values of temperature and relative humidity, when using the crystalline silicon modules. There are other researchers investigated different photovoltaic types to evaluated the performance in different environmental conditions such as in India, Pakistan, Peru, Greece, etc.[12-10]

In this research paper, it was achieved comparison between the performance of different PV modules to investigate the influence of operation parameters on the performance of the selected PV modules. Where these operation parameters are module temperature and irradiance intensity. Additionally, it was characterized the operating conditions of PV modules to understand deeply the influence of deviation from Standard Test Conditions (STC) on the performance of PV modules. All tests were achieved in Baghdad city (Iraq). The period of collected data (measurements) started from September 2020 and ended at May 2021 (approximately 7 months). The main aims of this work are firstly to characterize the working conditions at Baghdad city and secondly to show

the differences of performance of two types of PV module.

2. Experimental work

All the measurements in this research paper were performed at the University of Baghdad (Energy Eng. Dept.), Baghdad (Iraq), using the Photovoltaic Test facility (Outdoor). Where the experimental work performed on the roof of building of Energy Eng. Dept. with height 12 m. Where the location of the work at longitude (44° 25' 16" E) and latitude (33° 19' 34" N). Where the data that come from measurements of the selected PV modules can be obtained 24 hours a day using different types of atmospheric and irradiance sensors. Where the range of irradiance was between 500-1000 W/m2. In the experimental work, it was selected two different PV technologies. Where, the Thin Film Technologies represent were appeared in thin film family (amorphous silicon and copper indium gallium di-selenide) .

The PV modules are calibrated according to standard procedure available by the manufacturer depending on the measurements at STC (standard testing condition) solar irradiance (G) = 1000 W/m2 and cell temperature (TC)= 25 oC. Figure 1 shows the Prova 200 (Solar Panel analyzer) that was used for the measurements in the experiments. The main specifications of Solar Panel analyzer (Prova 200) list in Tables 1. It can be obtained very important results by using the Solar Panel analyzer such as maximum solar power, current and voltage. Furthermore, I-V curves cane be presented based on the results.

The two solar modules system is available in Figure 2, for Baghdad, for maximum output the module must have been south facing inclined with 33.3-degree angle to the horizontal. All the data are recorded just like the outdoors-monitoring system; recording module surface temperature, voltage divider circuit is used for recording voltage, and current sensor, operated using relay is used for measuring the currents, and all these data are recorded with the help of solar analyzer (Prova 200). Table 2 presents the main specifications of the selected solar modules.

Table 1. Specification of solar module analyzer (Prova 200)

Battery Type:	Rechargeable Lithium Battery (1600mAh)
AC Power Adapter:	0V input, DC 12V 2AC 100V~2 / 1~3A output
Data Logging Memory Size:	100 records
Dimension:	257 (L) x 155 (W) x 57 (H) mm 10.1" (L) x 6.1" (W) x 2.2" (H)
Weight:	1160g / 40.0oz (Batteries included)
Operation Environment:	5℃ ~ 50℃, 85% RH
Temperature Coefficient:	0.1% of full scale / ℃ (＜18℃ or ＞28℃)
Storage Environment:	-20℃ ~ 60℃, 75% RH
Accessories:	User manual x 1, AC power adapter x 1, Rechargeable lithium battery x 1, Optical USB cable x 1, Software CD x 1, Software manual x 1, Carrying bag x 1, Kelvin clips (2 clips, 6A max) x 1 set, 4-wire to 2-wire connector x 1 set

DC voltage measurement

Range	Resolution	Accuracy
0-0.6 mA	0.001 V	±1% ± (1% of Vopen ± 9mV)
6-10 V	0.001 V	±1% ± (1% of Vopen ± 0.09V)
10-60 V	0.01 V	±1% ± (1% of Vopen ± 0.09V)

Table 2. Modules specifications at STC as presented by the manufacturer.

	a-Si	CIGS
Area [m^2]	0.147	0.055
Voc [V]	27	3.5
I_{sc} [A]	0.35	2.7
V_m [V]	18	2.8
I_m [A]	0.227	2.5
P_m [W]	5	7
Ns	18	6

Figure 1. The Prova 200 solar panel

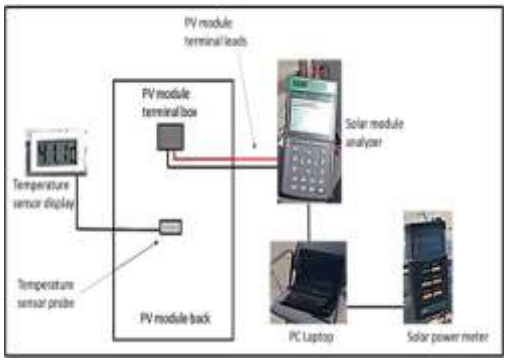

Figure 2. Solar module system.

3. Current-Voltage and Power-Voltage Characteristic

The most significant points that will specify the performance of I-V curve of PV module are the maximum-power point (MPP), open circuit and short circuit. It can be estimated the normal irradiance component (**G)** based on the data of the short-circuit current in case of uniform lighting. Where G is called also the in-plane irradiance or plane-of-module irradiance. Also, it can be found the effective operating temperature for modules based on the data of the open-circuit voltage (V_{OC}). Where, it's called the equivalent cell temperature (ECT). Furthermore, there are other important elements that affect the performance of the modules such as the instantaneous efficiency (η) of the maximum power point (MPP) and the fill factor (FF) that affected significantly the behavior of I-V curve. In case, when the magnitude of the fill factor is high then will lead the of I-V curve to be more rectangular in shape.

In the present research paper, it was achieved the experimental work in order to evaluate and analysis the performance two photovoltaic (PV) (Amorphous Silicon (a-Si) Copper Indium Gallium Diselenide (CIGS) technologies. In the second step, the comparisons were achieved between the two types. All tests were conducted out under the climate conditions of Baghdad city (Iraq). The elevation of the selected site is 9 m above ground level. The experimental work covered the eight commercially available PV technologies. It was employed two technologies in this work are; Amorphous Silicon (a-Si) and Copper Indium Gallium Diselenide (CIGS). The set of data analyzed in this paper was systematically acquired during a period of 7 months (starting Oct. 2020 to April 2021). Special attention is given to the influence of temperature and solar radiation the performance of the PV modules. The following results give a sample of results for a given days in select months.

Figures (3-6) show the results of the proposed experimental approach, where it can be seen the I-V and P-V for the two solar modules at solar radiations 750 W/m^2 and 1000 W/m^2 at September, 2020. Consequently, Figure 7 to Figure 10 show the I-V and P-V for the two solar modules at solar radiations 750 W/m^2 and 1000 W/m^2 at January, 2021. Tables 3 & 4 show the comparison between the proposed approach and the results of other researcher [15]. It can be seen the high agreement between the obtained results and results of other researchers that proved the accuracy of the results.

4. Measured Data Output

It was obtained all data of the experimental voltage, current and power as an Excel sheet from the software of the Solar Module Analyzer. Based on these data, it can be presented the curves of IV and PV. The electrical parameters of the two PV solar module, the solar module temperature and weather factors presented in Tables (3- 6) with constant radiation flux (750 and 1000 W/m²) for period (October 2020 to April 2021). Table 3 and Table 4 summarized electrical parameters, solar module temperature, weather factor, fill factor and efficiency of amorphous solar module while, Table 7 and Table 8 for CIGS solar module.

The maximum values of power (P_{max}) at solar radiation intensity 750 W/m² are 2.742, and 2.831 for amorphous silicon and copper indium gallium di-selenide respectively because we have the lowest solar module operating temperature (19 ^{o}C, 17 ^{o}C for solar radiation 750 and 1000 W/m^2 respectively) and ambient temperature (7 ^{o}C) and for Jan., 2021 than other months. Consequently, the same behavior for the two modules at solar irradiance 1000 W/m^2 with the highest power value; 2.680, and 3.198 of amorphous silicon and copper indium gallium di-selenide respectively.

Furthermore, the minimum values of power (P_{max}) at solar radiation intensity 750 W/m² are 2.530, and 2.831 for amorphous silicon and copper indium gallium di-selenide respectively because we have the highest solar module operating temperature (57 ^{o}C, and 55 ^{o}C respectively) and ambient temperature (45 ^{o}C) for April, 2020 than another month. Consequently, the same behavior for the two modules at solar irradiance 1000 W/m^2 with the highest power value; and 2.680, and 3.198 of amorphous silicon and copper indium gallium di-selenide respectively. The highest efficiency can be notes for CIGS solar module with a value 7.3%, while the lowest one is 5.5% for amorphous solar module.

5. Current-Voltage Characteristic Curve

In this section, it will present and discuss with details the I-V curve for all cases operating that works under normal conditions as shown in Figures 3, 5, 6 and 9. The lowest magnitude of current is equal to zero when the solar cell open-circuited is not connected to any load, where highest magnitude of voltage occurred across the cell. This is identified as solar cell open circuit voltage (V_{oc}). While, the lowest magnitude of voltage is equal to zero wen the it connected to loads (positive and negative). This is occurred when the the solar cell is short circuited. Where, the highest magnitude of current occurred. This is identified as solar cell short circuit current (I_{sc}). The range of I-V characteristics for solar cell is begin short circuit current (I_{sc}) when the output voltage is to the current when equal to zero in case of full open circuit voltage (V_{oc}). In other words, in case of open circuit, it can be obtained the maximum voltage, while in case of closed circuit, it can be obtained the maximum current. Obviously, there is no electrical energy can be obtained based on these two conditions, but there is a point within which these two points are possible for the solar cell to generate the maximum amount of power. Therefore, the ideal operation of a photovoltaic cell (or panel) is defined to be at the maximum power point. However, there is an optimal point that based on the specific combination of current (I_{mp}) and voltage (V_{mp}) that lead to generate the maximum power point (MPP). For this reason, the maximum power point presents the ideal operation of a photovoltaic cell.

It can be observed that the maximum power point (MPP) occurred nearby the bend of I-V characteristics curve. It can be found the

magnitudes of ($I_{mp} \cong 0.95\ I_{sc}$) and ($V_{mp} \cong 0.90\ V_{oc}$) from the short circuit current and open circuit voltage. It can be seen this behavior is satisfied in the present work (see Figures 3-10). Where, both of outputs (current and voltage) are function of temperature, this lead to make the output power will be varied according to the surrounding temperature.

Figures 3, 5, 7 & 9 illustrate the characteristics of I-V under different surrounding temperatures. It's clear that results curves of selected modules intersect each other at a specific point. Where, the PV cell short circuit current increased when the surrounding temperature increased too. While, PV cell open-circuit voltage decreased when the surrounding temperature increased. Figures 3 & 4 show the selected I-V characteristics with corresponding P-V characteristics simultaneously.

It can be proved the results based on the theoretical approach based on the band theory of solid-state physics as shown in Figure 11. It can be seen in Figure 11(a) the levels of energy of semiconductors (N-type and P-type). While, it can be seen in Figure 11(b) the equalization of Fermi energy and bands of PN junction in a non-illuminated photovoltaic cell. It was described the equilibrium state the currents of diffusion and ohmic. It can be seen in Figure 11(c) the condition of PV cell (after illuminating), if it's not connected to an electric circuit. Incident photons disturb the original equilibrium and establish a different equilibrium.

The generation of pairs (Electron-hole) will be accelerated (increased) in PN junction region, in electric field $E\rightarrow$ direction of arrows. N-type and P-type became charged negatively and positively, respectively. Where, the Fermi levels in regions of N-type and P-type will separate and the potential barrier V_D will decrease. Therefore, it can represent the voltage of photovoltaic V_P as potential difference between regions that explained in results. At most, this voltage could correspond with compensation of original bending of bands. Where, it's usually approximately equal to $V_P \approx 0.6$ V for silicon PV cell. The P and N regions and temperature paly important rule to specify the exact voltage value. Additional increment in the magnitude of irradiation intensity will not increase the the open-circuit voltage as shown in Figure 12, because there is a limit value of photovoltaic open-circuit voltage. This is happened when the potential of photovoltaic and opposing space charge balanced at the PN junction. The motion direction of holes and generated electrons will not be separated any more for PN junction. It can be explained the process as a reduction in potential barrier V_D as reducing the potential barrier V_D due to illumination that lead to rise the diffusion current of electrons into the P-type semiconductor. Then, it will increase the diffusion current of holes into N-type. Therefore, it can be compensated the increment in the current, that is happened due to the separation of generated electrons and holes in the electric field. The new equilibrium was founded due to the contribution of the voltage of photovoltaic. The magnitude of open-circuit voltage (limitary magnitude) corresponded with equalization of the original bending for bands in PN junction. This occurred in case when existing the highest separation of Fermi energy levels.

The photovoltaic voltage will be reduced when the illuminated PV cell connects to electric circuit. Therefore, repeated increments in the potential barrier (VD – VP) will be occurred due to the change in bands curvature. The separation of generated electrons and holes in electric field ($E\rightarrow$ between fixed space charges) will lead to decrease the values of currents of diffusion and predominates. The summation of both currents

has a certain value and not equal to zero any more.

The electric circuit will be supplied with the resulting current, where the sources is the PV cell. In case, when the temperature is constant and the resistance in the circuit reduces (from infinite to zero), due to this situation the source's operating point will be moved along the curve from open-circuit voltage to short-circuit current as shown in Figures 3, 5, 7 and 9. It can be seen the Optimal operating points (arrows on the curves), and it can be found the rectangle area by axes and largest working point, therefore the source will provide the maximum power in electric circuit (Figures 3 & 5 or Figures 7 & 9). The level of Fermi energy will be shifted to forbidden gap center and the gap narrows when the temperature increases as shown in Figure 12. It's obvious from the Figures 11(c) & 12, that the decreased of photovoltaic voltage Vp at constant irradiation intensity occurred due to the increases temperature.

At the same time, the forbidden gap in the band structure of energy levels will be narrower when the temperature is high. Where this will affect the higher generation of electron-hole pairs in illuminated PN junction and lead to grow the magnitude of current. Where, there is a correspond between the maximum area and the amount of reduction in the maximum power supply by the PV cell. Therefore, the efficiency of energy conversion for photovoltaic will be decrease with increases of the temperature of PV cells. The values of conversion efficiency will approach to zero when the temperature of PV cell is equal approximately 500 K.

Table 3. Comparisons of the proposed electrical solar parameters of amorphous photovoltaic module with Ref. [15] at constant radiation 700W/m².

	T_c/℃	T_a/℃	u/m/s	P_{max}/W	V_{max}/A	I_{max}/V	η/%	F.F
Oct.,2020	47	38	1.8	2.530	14.903	0.169	4.2	0.555
Oct., 2016 [15]	48	37	2.2	2.482	14.723	0.168	4.1	0.533
Jan.,2021	23	14	4.0	2.742	15.128	0.180	4.0	0.400
Jan., 2016 [15]	19	12	2.5	2.688	14.782	0.181	4.2	0.406

Table 4. Comparisons of the proposed electrical solar parameters of CIGS photovoltaic module with Ref. [15] at constant radiation 700W/m².

	T_c/℃	T_a/℃	u/m/s	P_{max}/W	I_{max}/A	V_{max}/V	η/%	F.F
Oct.,2020	47	38	1.8	2.831	1.901	1.488	5.5	0.567
Oct., 2016 [15]	48	37	2.2	2.811	1.892	1.486	5.7	0.588
Jan.,2021	23	14	4.0	3.184	2.131	1.483	6.2	0.617
Jan., 2016 [15]	19	12	2.5	3.165	2.100	1.507	6.0	0.614

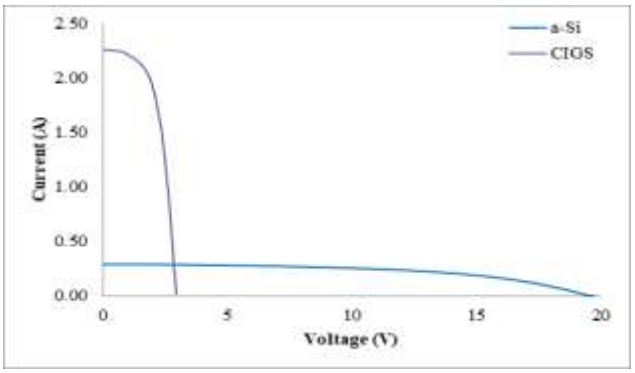

Figure 3. I-V characteristic curves of the two test solar modules at solar radiation 750 W/m^2 at September, 2020

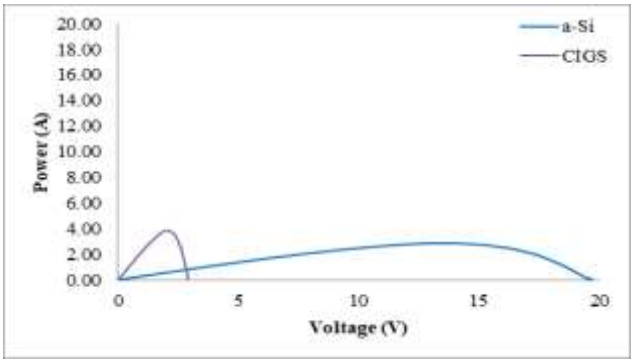

Figure 4. P-V characteristic curves of the two test solar modules at solar radiation 750 W/m^2 at September, 2020

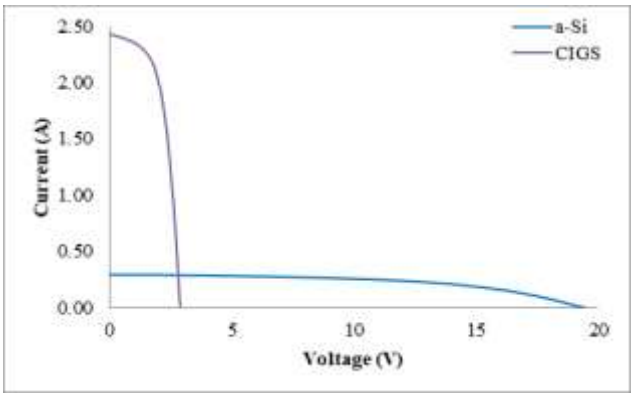

Figure 5. I-V characteristic curves of the two test solar modules at solar radiation 1000 W/m^2 at September, 2020

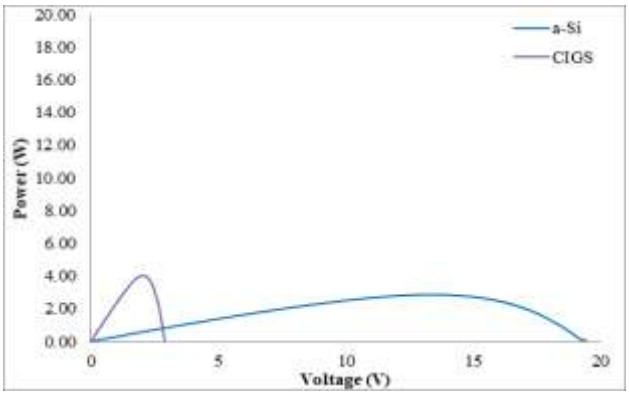

Figure 6. I-V characteristic curves of the two test solar modules at solar radiation 1000 W/m^2 at September, 2020.

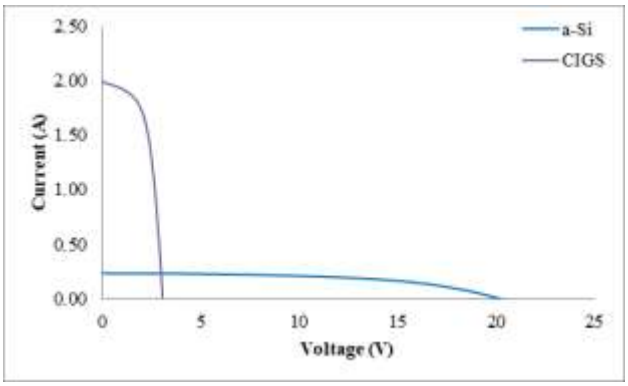

Figure 7. I-V characteristic curves of the two test solar modules at solar radiation 750 W/m^2 at January, 2021.

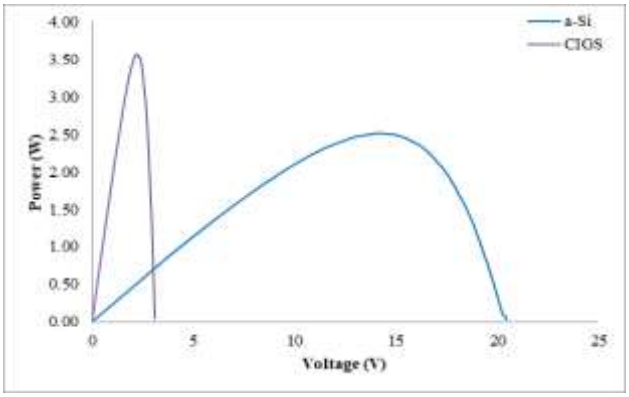

Figure 8. P-V characteristic curves of the two test solar modules at solar radiation 750 W/m^2 at January, 2021

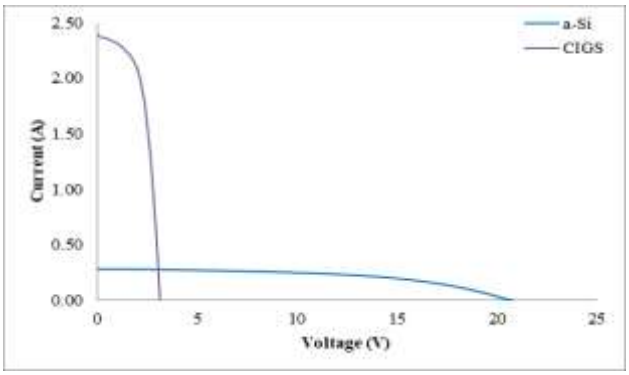

Figure 9. I-V characteristic curves of the two test solar modules at solar radiation 1000 W/m^2 at January, 2021

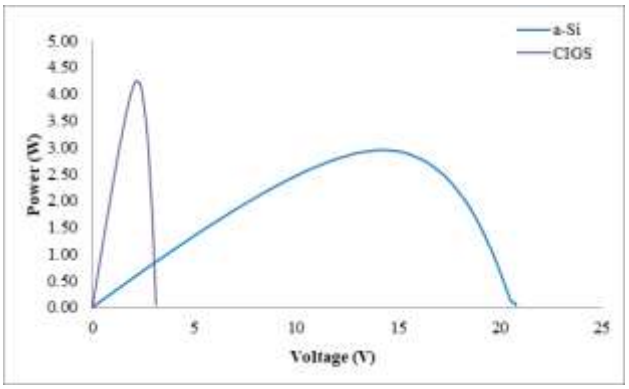

Figure 10. P-V characteristic curves of the two test solar modules at solar radiation 1000 W/m^2 at January, 2021

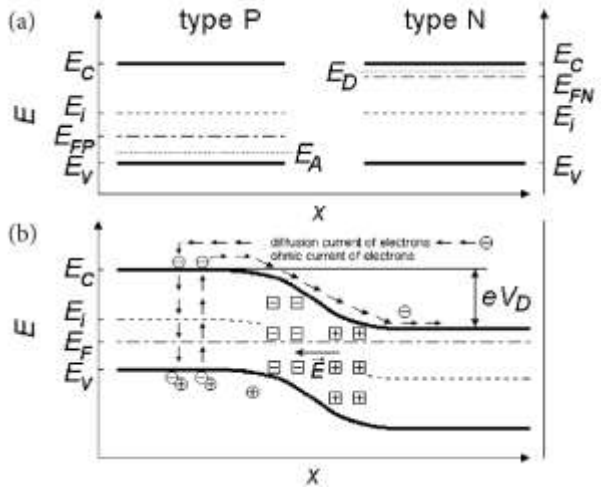

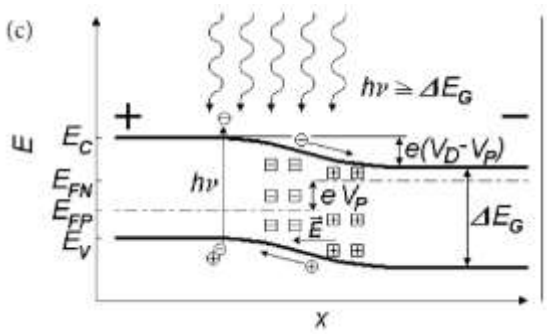

Figure 11. The energy levels: (a) semiconductor type P, N, (b) not illuminated PN junction, and (c) illuminated PN junction [13]

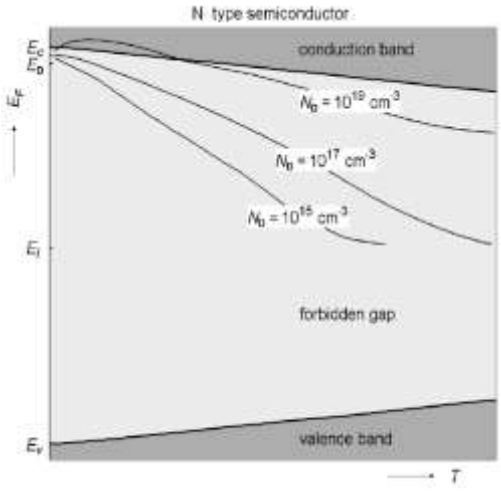

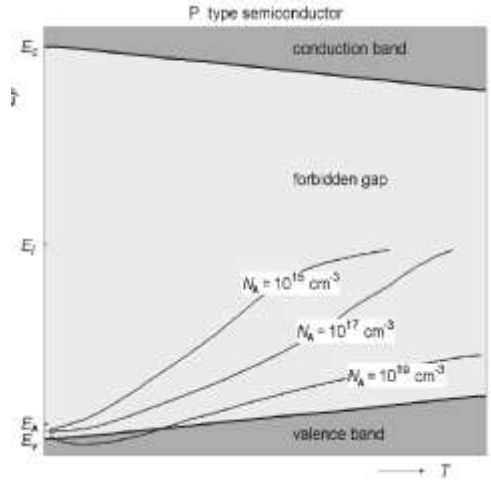

Figure 12. Dependence of the Fermi energy level and forbidden band width (energy gap) on temperature at three dopant [14] concentrations [9].

6. Conclusions

In this research paper, a new approach was developed based on a simple I-V curve tester for PV modules. The results proved that the proposed system was successed experimentally to extract I-V curves of the two selected PV modules (amorphous and CIGS solar modules). The maximum values of power (P_{max}) at solar radiation intensity 750 W/m² are 2.742 W, and 2.831 W for amorphous silicon and copper indium gallium di-selenide respectively because we have the lowest solar module operating temperature (19 ^{o}C, 17 ^{o}C for solar radiation 750 and 1000 W/m^2 respectively), and ambient temperature (7 ^{o}C) and for Jan., 2021 than other months. Consequently, the same behavior for the two modules at solar irradiance 1000 W/m^2 with the highest power value; 2.680 W, and 3.198 W of amorphous silicon and copper indium gallium di-selenide respectively.

Furthermore, the minimum values of power (P_{max}) at solar radiation intensity 750 W/m² are 2.530, and 2.831 W for amorphous silicon and copper indium gallium di-selenide respectively because they have the highest solar module operating temperature (57 ^{o}C, and 55 ^{o}C respectively) and ambient temperature (45 ^{o}C) for April, 2020 than other months. Consequently, the same behavior for the two modules at solar irradiance 1000 W/m^2 with the highest power value; and 2.680 W, and 3.198 W of amorphous silicon and copper indium gallium di-selenide respectively. The highest efficiency can be notes for CIGS solar module with a value 7.3 %, while the lowest one is 5.5% for amorphous solar module.

Acknowledgements

This work funded by University of Baghdad. Also, the authors would like to thank the System Technology and Mechanical Design Methodology Group / Hamburg University of Technology to support this research paper.

Conflict of Interest

The authors declare that there are no conflicts of interest regarding the publication of this manuscript.

7. References

1. Kai Maraun and Akane Yamiya, 2015. Solar Frontier Achieves World Record Thin-Film Solar Cell Efficiency: 22.3 http://www.solar-frontier.com/eng/news/2015/C051171.html.
2. Yousaf H. Khattak, 2019, Modeling of High-Power Conversion Efficiency Thin Film Solar Cells, Ph. D. thesis, Universitat Politècnica de València.
3. Pizzini, S. (Ed.). (2012). Advanced silicon materials for photovoltaic applications. John Wiley & Sons.
4. Rein, S., 2006. Lifetime spectroscopy: a method of defect characterization in silicon for photovoltaic applications (Vol. 85). Springer Science & Business Media.
5. Tiwari, Gopal Nath, and Swapnil Dubey. Fundamentals of photovoltaic modules and their applications. Royal Society of Chemistry, 2009.
6. Panasonic. Panasonic HIT™, 2016. http://panasonic. net/ecosolutions/solar/hit/.
7. William N. Shafarman, Susanne Siebentritt, and Lars Stolt. 2011, Handbook of Photovoltaic, Science and Engineering. John Wiley & Sons, Ltd, 2nd edition.
8. Katee Narjes, Abdullah Oday I, Hashim Emad T., 2021, "Extracting Four Solar Model Electrical Parameters of Mono-Crystalline Silicon (mc-Si) and Thin Film (CIGS) Solar Modules using Different Methods", Journal of Engineering, Number 4 Volume 27.
9. Tossa, Alain K., Soro, Y.M., Thiaw, L., Azoumah, Y., Sicot, Lionel, Yamegueu, D., Lishou, Claude, Coulibaly, Y., Razongles, Guillaume, 2016. Energy performance of different silicon

photovoltaic technologies under hot and harsh climate. Energy 103, 261.

10. Magare, D.B., Sastry, O.S., Gupta, R., Betts, T.R., Gottchalg, R., Kumar, A., Bora, B., Singh, Y.K., 2016. Effect of seasonal variations on performance of three different photovoltaic technologies in India. Int. J. Renew. Energy Environ. Eng. 7, 93–103.
11. Gaglia, A.G., Lykoudis, S., Argiriou, A.A., Balaras, C.A., Dialynas, E., 2017. Energy efficiency of PV panels under real outdoor conditions—An experimental assessment in Athens, Greece. Renew. Energy 101, 236-243.
12. Romero-Fiances, I., Muñoz-Cerón, E., Espinoza-Paredes, R., Nofuentes, G., de la Casa, J., 2019. Analysis of the performance of various PV module technologies in Peru. Energies 12, 186.
13. Frank H., Snejdar V. 1976: Principy a vlastnosti polovodičových součástek. Prague, SNTL.
14. Hieslmair H., Istratov A.A., Flink C., McHugo S.A., Weber E.R. 1999: Experiments and computer simulations of iron profiles in p/p+ silicon: segregation and the position of the iron donor level. Physica B, 273–274: 441–444.
15. Abdulameer A. Akram., "Temperature Effect on Power Drop of Different Photovoltaic Modules", MSc. Thesis, Baghdad University, 2016.